

# Thunderstorms Increase Mercury Wet Deposition

Christopher D. Holmes,<sup>\*,†</sup> Nishanth P. Krishnamurthy,<sup>†</sup> Jane M. Caffrey,<sup>‡</sup> William M. Landing,<sup>†</sup> Eric S. Edgerton,<sup>§</sup> Kenneth R. Knapp,<sup>||</sup> and Udaysankar S. Nair<sup>⊥</sup>

<sup>†</sup>Department of Earth, Ocean, and Atmospheric Science, Florida State University, Tallahassee, Florida 32306, United States

<sup>‡</sup>Center for Environmental Diagnostics and Bioremediation, University of West Florida, Pensacola, Florida 32514, United States

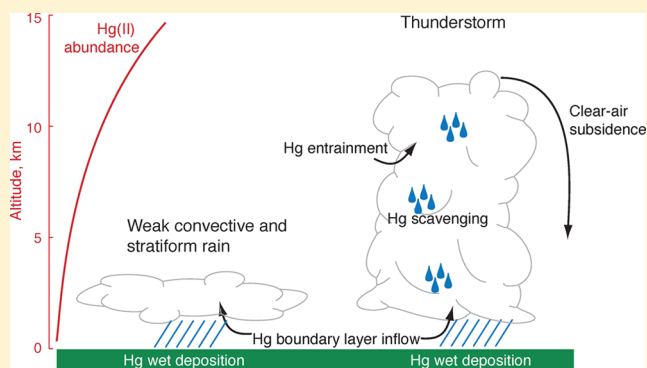
<sup>§</sup>Atmospheric Research & Analysis, Inc., Cary, North Carolina 27513, United States

<sup>||</sup>National Centers for Environmental Information, National Oceanic and Atmospheric Administration, Asheville, North Carolina 28801, United States

<sup>⊥</sup>Department of Atmospheric Science, University of Alabama, Huntsville, Alabama 35805, United States

## S Supporting Information

**ABSTRACT:** Mercury (Hg) wet deposition, transfer from the atmosphere to Earth's surface by precipitation, in the United States is highest in locations and seasons with frequent deep convective thunderstorms, but it has never been demonstrated whether the connection is causal or simple coincidence. We use rainwater samples from over 800 individual precipitation events to show that thunderstorms increase Hg concentrations by 50% relative to weak convective or stratiform events of equal precipitation depth. Radar and satellite observations reveal that strong convection reaching the upper troposphere (where high atmospheric concentrations of soluble, oxidized mercury species (Hg(II)) are known to reside) produces the highest Hg concentrations in rain. As a result, precipitation meteorology, especially thunderstorm frequency and total rainfall, explains differences in Hg deposition between study sites located in the eastern United States. Assessing the fate of atmospheric mercury thus requires bridging the scales of global transport and convective precipitation.



## 1. INTRODUCTION

For 20 years, the Mercury Deposition Network (MDN) has recorded mercury content of precipitation across North America.<sup>1</sup> During this period, states bordering the Gulf of Mexico consistently receive the highest mercury wet deposition in the eastern United States (Figure 1), typically about double that of the Northeast states<sup>2,3</sup> despite lower anthropogenic mercury emissions in the Southeast (Figure S1).<sup>4–6</sup> On a seasonal basis, deposition peaks in summer, which coincides with frequent deep convective rainstorms. Guentzel et al.<sup>7</sup> found that summer rainwater mercury concentrations are uniformly high across Florida, leading them to hypothesize that convective rain scavenges soluble Hg(II) from a widespread reservoir in the free troposphere. This high-altitude Hg(II) reservoir may be supplied to the Gulf Region by oxidation of Hg(0) in the upper troposphere, followed by subsidence in the subtropical highs, the descending branch of the Hadley circulation.<sup>8</sup> Aircraft have observed high Hg(II) over the southeast United States,<sup>9–12</sup> and back trajectories attribute it to subsidence.<sup>11–13</sup> Despite the hypothesized role of thunderstorms in tapping this high-altitude Hg(II), no direct tests of this mechanism have been made to date, which is the goal of this work.

Thunderstorms are deep convective rainstorms whose intense updrafts reach above 10 km in the eastern United States.<sup>14</sup> Within the cloud and updrafts, condensed water and ice efficiently scavenge soluble gases and aerosols, such as Hg(II).<sup>15</sup> Thunderstorms can scavenge Hg(II) from the boundary layer through air convergence into the cloud base and from high altitudes by lateral entrainment into the buoyant cloud. Weak and nonconvective rain events, in contrast, have lower maximum altitudes and can only scavenge from the lower troposphere.

We investigate the role of thunderstorms and Hg wet scavenging in the free troposphere by compiling a large data set of Hg measurements in rainwater from individual storms at multiple sites (Figure 1). The sites span the north–south gradient of Hg deposition, allowing comparisons of high- and low-deposition environments. We focus on rain events during June–August to understand the peak deposition season and to avoid confounding seasonal changes in meteorology, emissions,

Received: May 23, 2016

Revised: July 27, 2016

Accepted: July 27, 2016

Published: July 27, 2016

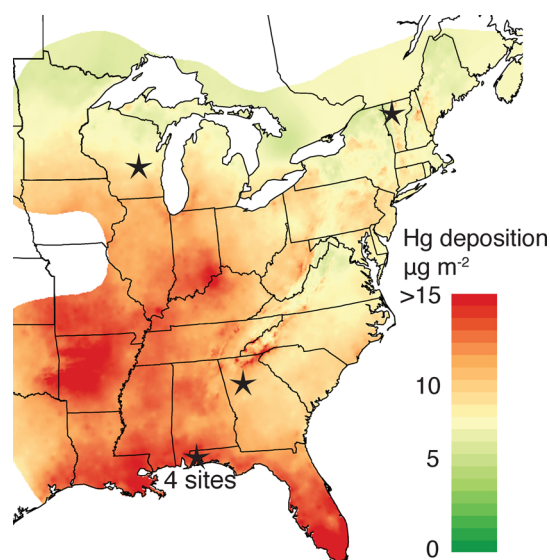


**Figure 1.** Mean annual mercury wet deposition in the eastern United States in 2006–2011,<sup>1</sup> with stars marking the locations of seven sites (Tables 1 and S1) analyzed here. The deposition map represents the regional background and does not resolve high Hg wet deposition in some urban areas and near some large point sources.

and atmospheric chemistry. Using individual storm (i.e., event) samples, rather than more-common weekly or monthly samples, is essential for discerning the meteorological and chemical processes that influence scavenging and deposition. After identifying thunderstorm events, we use a statistical model to show that, at all study sites, rainwater from thunderstorms has higher Hg concentrations than other storms with equal rainfall. Satellite infrared imagery, ground-based radar, and ground-level atmospheric Hg(II) measurements provide further evidence that the main source of Hg(II) scavenged by these storms originates in the free troposphere. Because wet deposition is the product of Hg concentration and precipitation depth, we use the statistical model to quantify how differences in thunderstorm frequency, total precipitation, and the atmospheric supply of Hg(II) contribute to different Hg wet deposition at the study sites, including the high deposition around the Gulf of Mexico.

## 2. MATERIALS AND METHODS

**2.1. Hg Observations and Site Descriptions.** This study examines seven sites in the eastern United States (Figure 1 and

Tables 1 and S1) where mercury concentrations in individual rain events ( $n = 817$ ) were measured. We began with four sites near Pensacola, FL that were operated by the coauthors during the summers of 2006–2011.<sup>16,17</sup> To assess regional differences in Hg concentration and deposition, we added all sites from the public MDN archive that measured individual rain events during those years. A total of three MDN sites met those criteria: Devil's Lake, WI; Underhill, VT; and Yorkville, GA.<sup>1,2</sup> Some MDN sites have collected event samples in other years, but they are excluded to avoid the confounding effects of interannual variability or trends in meteorology, emissions and atmospheric chemistry. All sites comply with MDN protocols for distance from interfering structures, clean sample collection, and mercury analysis by atomic fluorescence.<sup>2,17</sup> MDN data were downloaded from the National Atmospheric Deposition Program (NADP) archive,<sup>1</sup> and other Hg deposition data were provided by the site investigators. Samples with MDN quality code "C" are invalid and excluded from further analysis. Missing or invalid data comprised <15% of summer days at all sites in all years, except the Georgia site in 2006 that began event sampling in August of that year. Overall, fewer than 5% of days are missing, and these should not affect our regression analysis. Our data set encompasses the majority of summer mercury deposition at these sites because wet deposition is typically 60–90% of total Hg(II) deposition in the eastern United States, except near some large point sources.<sup>5,18–21</sup>

The seven sites collected 817 summer precipitation samples during the years of 2006–2011, of which 413 are from the Pensacola area. Mercury deposition totaled 5.3–5.7  $\mu\text{g m}^{-2}$  at the Florida sites each summer season, with substantial (1–2  $\mu\text{g m}^{-2}$ ) interannual variability. Previous analysis of the Pensacola sites, which is confirmed by our Table 1, showed that Hg concentration, deposition, and precipitation are statistically indistinguishable among these four sites and other MDN sites in the northern Gulf of Mexico region despite some sites being near urban and point sources;<sup>22</sup> summer precipitation and Hg deposition rise further in South Florida, however (Figure 1). The Pensacola sites are 10 to 40 km away from the ocean, and wet deposition of sea salt ions (e.g., sodium and chloride) decreases over this distance,<sup>22</sup> but there is no trend in Hg concentration or deposition (Table 1). Figure 2 shows a smooth distribution of precipitation depths and Hg concentrations across the four Florida sites, so we treat them all as samples from a single statistical population in the analysis below.

**Table 1. Summary of Mercury Wet Deposition Events for June–August of 2006–2011<sup>a</sup>**

site (MDN code)	summer precipitation samples	summer precipitation, mm <sup>b</sup>	summer deposition, $\mu\text{g m}^{-2b}$	summer concentration, $\text{ng L}^{-1bc}$	deposition per summer event, $\text{ng m}^{-2d}$
Ellyson Field, Pensacola, FL	92	450 ± 130	5.4 ± 1.2	12.2 ± 2.3	340 ± 230
Pace site, Pensacola, FL	81	460 ± 120	5.8 ± 1.8	13.1 ± 4.4	420 ± 390
Molino site, Pensacola, FL	81	420 ± 100	5.5 ± 1.8	12.9 ± 2.1	400 ± 350
Outlying Landing Field, Pensacola, FL (FL96)	159	500 ± 60	5.7 ± 0.8	11.5 ± 1.9	240 ± 200
Pensacola, FL (all combined)	413	460 ± 100	5.6 ± 1.4	12.4 ± 2.9	330 ± 300
Yorkville, GA (GA40)	109	310 ± 73	3.9 ± 0.3	12.9 ± 2.9	200 ± 200
Devil's Lake, WI (WI31)	145	410 ± 200	4.8 ± 1.9	12.3 ± 3.2	220 ± 270
Underhill, VT (VT99)	150	450 ± 90	4.0 ± 1.1	9.1 ± 3.6	160 ± 190

<sup>a</sup>Table S1 provides geographic coordinates and additional site information. <sup>b</sup>Values are interannual mean of seasonal (June–August) totals and interannual standard deviation of seasonal totals. <sup>c</sup>Volume-weighted mean concentration. <sup>d</sup>Mean and standard deviation, excluding trace precipitation events.

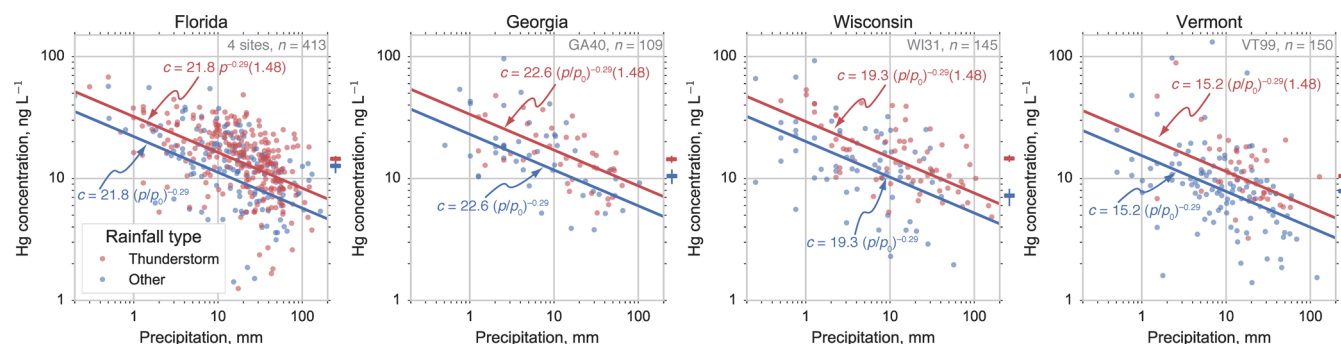


**Figure 2.** Mercury concentration in summer precipitation (June–August), classified by storm type. Lines show fit with eq 1, and bars on the right vertical axis of each panel show the mean and standard error for precipitation events exceeding 10 mm. The inset text site gives MDN site codes, where applicable, and the number of precipitation samples.

The Georgia site has the lowest summer Hg deposition of any site here ( $3.9 \pm 0.3 \mu\text{g m}^{-2}$ ); section 3.3 shows that the low deposition is due to having the least summer precipitation because the mean Hg concentration is exceeded only at the Florida sites. Summer Hg deposition is  $4.8 \pm 1.9 \mu\text{g m}^{-2}$  at the Wisconsin site and  $4.0 \pm 1.1 \mu\text{g m}^{-2}$  at the Vermont site. Prior studies found that these sites have similar Hg concentrations, trends, and precipitation to other rural sites in the Great Lakes and New England regions, respectively.<sup>2,6,23–25</sup> In addition, there are no sharp precipitation gradients or topographic features near any of the sites that are expected to make them atypical of their regions (Figure S2). At all sites, there are occasionally (1–2 times per summer) large precipitation events that can deposit as much as 20–30% of the mean summer Hg wet deposition flux. The largest 10 Hg deposition events at all sites are thunderstorms, except in Vermont, where only half are thunderstorms (classification explained below). While these events are large, they are not outliers from the overall distribution of precipitation events shown in Figure 2, so they do not have excessive or suppressed influence on the statistical results below.

One of the Pensacola area sites continuously monitors concentrations of gaseous and fine particle-bound Hg(II), which, along with coarse particle-bound Hg(II), can all be scavenged by precipitation. The site also measures gaseous elemental mercury (Hg(0)), but this has very low solubility in water and does not contribute to wet deposition. Measurements are made hourly with an automated Tekran 2537/1135/1130 speciation unit.<sup>16</sup> Mean summer Hg(II) concentrations (excluding coarse particles that were not measured) during the study period were  $4.05 \text{ pg m}^{-3}$ , and Hg(0) was  $1.25 \text{ ng m}^{-3}$  (Table S2), similar to past measurements at the site and in the region.<sup>21,26</sup> Average Hg(II) concentrations were also calculated during each precipitation sample collection at the site.

**2.2. Weather, Satellite, and Radar Data Sources.** Hourly weather reports from the nearest Automated Surface Observing System (ASOS) were extracted from the Weather Underground Historical Weather archive (<http://www.wunderground.com/history/>, accessed July 13, 2013). These ASOS sites are listed in Table S1. Precipitation samples are classified as a thunderstorm if thunderstorm or lightning activity were reported at the ASOS site or in the vicinity during the time that the precipitation sample was collected.

The GridSat-B1 (version 2) product from NCEI (<http://www.ncdc.noaa.gov/gridsat>, accessed July 23, 2013) provides quality-controlled infrared brightness temperatures from geostationary satellite instruments. Infrared ( $11 \mu\text{m}$ ) brightness

temperature, which is continuously observed by geostationary satellites, is a proxy for cloud-top height, with cold temperatures indicating high-altitude clouds.<sup>27</sup> We average brightness temperature from GridSat-B1 over a 12 km radius surrounding each rain collection site and attribute the precipitation to the coldest temperature (highest cloud) observed during sample collection.

Brightness temperatures can be biased low if a cold, nonprecipitating cirrus cloud obscures a shallow raincloud below it, so we also use radar reflectivity (Weather Surveillance Radar 1988 Doppler, WSR-88D), which detects the hydrometeors that cause scavenging and deposition.<sup>28,29</sup> Although hydrometeor concentration, type, and precipitation rate can be estimated from radar reflectivity, here we use only the reflection strength and height as indicators of the storm structure. We average the following standard radar products in a 12 km radius around each precipitation collection site during times when the radar detected precipitation at the site: reflectivity at base (lowest radar elevation angle), low (0–7 km), middle (7–10 km), and high (>10 km) altitudes and echo tops (the highest altitude where precipitation is detected). Table S1 lists the radars that are used. Radar data are from the National Centers for Environmental Information (<http://www.ncdc.noaa.gov/nexradinv/>, accessed July 4, 2013) and converted to netCDF format with the NOAA Weather and Climate Toolkit.

All data streams were merged using the dates and times when the wet deposition collectors were deployed and retrieved to determine the weather conditions when precipitation was collected.

**2.3. Regression Model.** Concentrations of many elements and ions in rain are commonly observed to follow a power law of precipitation depth;<sup>30–32</sup> adding storm type is an innovation in this work. Our regression model is

$$c = \beta_0(p/p_0)^{\beta_1}(1 + \beta_2S) \quad (1)$$

where  $c$  is Hg concentration in rainwater,  $p$  is precipitation depth,  $p_0 = 1 \text{ mm}$  is a constant,  $S$  is a categorical variable for storm type ( $S = 1$  for thunderstorm, 0 otherwise), and  $\beta_i$  ( $i = 0, 1, 2$ ) indicates fit parameters. With these definitions,  $\beta_0$  is the expected baseline concentration in a nonthunderstorm rain event with precipitation depth  $p_0 = 1 \text{ mm}$ ;  $\beta_1$  quantifies the dilution or washout effect in which concentration decreases  $(\exp(\ln(2)\beta_1) - 1) \times 100\%$  for each doubling of precipitation depth; and  $\beta_2$  is the fractional increase in concentration in a thunderstorm compared to that in a nonthunderstorm event with equal precipitation depth. The relationship between concentration, precipitation depth, and storm type in eq 1 is

Table 2. Predictors of Hg Concentration in Rainwater

predictor	value <sup>a</sup>	P <sup>b</sup>
baseline concentration, $\beta_0^c$		
Florida	21.8 ± 1.3 ng L <sup>-1</sup>	<0.001
Georgia	22.6 ± 1.8 ng L <sup>-1</sup>	<0.001
Wisconsin	19.3 ± 1.4 ng L <sup>-1</sup>	<0.001
Vermont	15.2 ± 0.9 ng L <sup>-1</sup>	<0.001
precipitation depth, $\beta_1^d$	-0.29 ± 0.02 (-18 ± 1% for doubling p)	<0.001
storm type, $\beta_2^e$	+0.48 ± 0.07	<0.001
satellite and radar variables, $\beta_3^f$		
cloud-top temperature	-0.005 ± 0.002 K <sup>-1</sup>	0.01
radar echo top	+0.043 ± 0.020 km <sup>-1</sup>	0.03
high-level reflectivity	+0.020 ± 0.009 dBZ <sup>-1</sup>	0.04
mid-level reflectivity	+0.011 ± 0.008 dBZ <sup>-1</sup>	0.15
low-level reflectivity	-0.006 ± 0.007 dBZ <sup>-1</sup>	0.39
base reflectivity	-0.006 ± 0.005 dBZ <sup>-1</sup>	0.31

<sup>a</sup>Best estimate and standard error from the regression model (eq 1) fitted to data shown in Table 1 and Figure 2. <sup>b</sup>P is the significance level (two-sided *t* test). <sup>c</sup>Expected concentration in nonthunderstorm rain events with 1 mm of precipitation. <sup>d</sup>The percent change in concentration per doubling of precipitation depth is  $(\exp(\ln(2)\beta_1)-1) \times 100\%$ . <sup>e</sup>The fractional increase in concentration in thunderstorms compared to other rain events of the same precipitation depth. <sup>f</sup>Effect of individual satellite or radar variables after controlling for baseline concentration, precipitation depth, and storm type. Units are fractional change in Hg concentration per unit change in *V*. For example, Hg concentration decreases 0.5% for each 1 K increase ( $= -0.005 \text{ K}^{-1}$ ) in cloud-top temperature.

nonlinear, but the log transformation is linear (see eq S1), which enables ordinary least-squares fitting. Fit residuals are found to be log-normally distributed (Figure 2), which supports the functional form of the regression equation. Statistical and graphical data analysis was conducted with pandas and statsmodels in Python 3.5.

In an initial analysis of Florida sites alone, all parameters,  $\beta_i$  ( $i = 0, 1, 2$ ), were statistically significant ( $P < 0.001$ ), while interaction terms between the  $\beta_i$  parameters were not ( $P \approx 0.5$ ). In particular, this means that the dilution parameter  $\beta_1$  does not depend on storm type. In a sensitivity test in which  $\beta_0$  was fitted separately for each of the four Florida sites, the baseline concentrations were statistically indistinguishable ( $P \approx 0.25$ ), consistent with the statistically identical Hg concentrations and deposition at these sites (Table 1).<sup>22</sup> Therefore, we pool all Pensacola area data for the rest of the analysis. We next fit each site outside Florida with eq 1 and find significant increases in Hg concentrations during thunderstorms at all sites (Figure 2). Furthermore, the dilution ( $\beta_1$ ) and thunderstorm ( $\beta_2$ ) parameters at all sites overlap the Florida values (68% confidence intervals,  $P > 0.32$ ), while the northern sites have significantly lower baseline concentrations ( $\beta_0$ ). Therefore, we can regress all observations from all sites with common dilution ( $\beta_1$ ) and thunderstorm ( $\beta_2$ ) parameters and site-specific baseline concentrations ( $\beta_{0,x}$  where  $x$  is the site). Finally, to test whether additional cloud properties correlate with Hg concentration, each is added individually to eq 1 as a multiplicative term  $(1+\beta_3)^V$ , where  $V$  is any one of the satellite or radar variables listed in section 2.1 and Table 2, and fit parameter  $\beta_3$  is the fractional change in Hg concentration per unit of  $V$ .

### 3. RESULTS AND DISCUSSION

**3.1. Thunderstorm and Dilution Effects on Hg Concentration.** Figure 2 shows the higher mercury concentrations found in thunderstorms. For any precipitation depth, the highest concentrations consistently occur in thunderstorms, while the smallest concentrations occur in other rain types, which include stratiform and weak convective rainfall. In

addition, concentrations decline with precipitation amount, reflecting a dilution effect that is common for soluble gases and aerosols.<sup>7,30,31</sup> Thunderstorms tend to have larger precipitation depth (Figure S3) and, therefore, greater dilution than other rain storms, so the elevated Hg concentration in thunderstorms are obscured if we average many events with different precipitation depths. At all Pensacola sites, for example, the mean concentration in large (>10 mm) rain events is  $13.7 \pm 0.5 \text{ ng L}^{-1}$  (SE;  $n = 250$ ) for thunderstorms versus  $12.3 \pm 1.4 \text{ ng L}^{-1}$  ( $n = 33$ ) for other storms. Figure 2 (bars) shows that thunderstorms have elevated Hg concentrations at all other sites as well, but the effect often appears only marginally significant when we calculate an average across rain depths. This demonstrates the importance of controlling for the dilution effect, as is done in the regression model, when assessing the effect of thunderstorms on Hg concentration.

We use multivariate regression to quantify the thunderstorm effect on Hg concentration while controlling for dilution effects and site differences. Regression results in Table 2 show that thunderstorms increase Hg concentration by 48% compared to other storms that produce the same amount of rain (95% confidence interval: 33–63%). In addition, Hg concentrations decline 18% for each doubling of rain depth (95% CI: 16–21%). The northern sites also have 15–30% lower baseline Hg concentrations than Florida and Georgia. There are no statistically significant differences in dilution between the storm types ( $P = 0.4$ , two-sided *t* test), no differences in the dilution effect across sites ( $P = 0.5$ – $0.9$ ), and no differences in the thunderstorm effect across sites ( $P = 0.16$ – $0.4$ ). Thus, the meteorological effects of dilution and thunderstorms on Hg concentration appear uniform across all of the study sites; the only difference is the lower baseline concentration at the northern sites. Overall, the regression model explains 33% of the observed concentration variance in precipitation, which is highly significant ( $P < 0.001$ , goodness-of-fit *F* test). Uncertainties in measuring Hg concentration in rainwater (10–15%<sup>2,17</sup>) contribute modestly to the unexplained variance, and some precipitation events could be misclassified if conditions at the collection site differ from the nearest airport.

The remaining unexplained variance is likely due to spatial heterogeneity within each storm; meteorological variation within the two broad storm classes, which is explored below; and day-to-day differences in the ambient atmospheric Hg(II) that is entrained into storms. For weak and nonconvective rain, some of this daily variability may be due to depletion of atmospheric Hg(II) by prior rain, although the effect does not rise to the customary 95% confidence level. In these events, Hg concentrations rise 3.6% for each day elapsed since a prior rain event ( $P = 0.06$ ; 95% CI:  $-0.1$ – $7\%$ ), indicating that the Hg(II) reservoir in the lower troposphere may require time to accumulate. Thunderstorms do not exhibit this behavior ( $P = 0.8$ ), suggesting that they scavenge from a different, larger Hg(II) reservoir that is quickly replenished.

### 3.2. Radar and Satellite Constraints and Scavenging

**Altitudes.** The regression model is consistent with thunderstorms increasing Hg deposition in Florida but does not reveal where the mercury in these rainstorms originates. To discriminate whether the Hg(II) scavenged by thunderstorms originates in the boundary layer or free troposphere, we use satellite and radar observations of convection height and strength. Table 2 shows that cloud properties at high altitudes correlate with Hg concentration in surface rain, while the low-altitude properties do not. Hg concentration increases 4% for every 1 km increase in precipitation echo top, the highest altitude at which precipitation is detected (95% CI:  $0$ – $8\%$   $\text{km}^{-1}$ ), after controlling for storm type, dilution effect, and site differences. This increase with altitude is in addition to the 50% concentration increase in thunderstorms. Others previously showed that monthly rainfall Hg concentrations correlate with monthly maximum echo top, but that result mainly reflects the common seasonal cycles of both variables, not the effect of individual storms, so their results are not comparable to ours.<sup>33</sup> If we approximate upper tropospheric temperatures with a dry adiabatic lapse rate, the satellite IR temperatures imply a 5% increase in Hg concentration for every 1 km increase in cloud top (95% CI:  $1$ – $9\%$   $\text{km}^{-1}$ ), similar to the precipitation echo tops. Large reflectivity and hydrometeor concentration at high altitudes ( $>10$  km) is also associated with high Hg concentration in precipitation ( $P = 0.04$ ), but hydrometeor concentrations at all lower altitudes have no such association ( $P = 0.15$ – $0.4$ ).

Large low-level hydrometeor concentrations are sustained by air and moisture inflow to the cloud base, so the radar data are inconsistent with a dominant Hg(II) source in the boundary layer. Rather, the radar and satellite data imply that Hg concentration in rain is most sensitive to convection reaching the upper troposphere, where independent observations have found high atmospheric Hg(II) concentrations.<sup>9,10,12,34–36</sup> These results are consistent with our previous numerical simulations showing that strong thunderstorms should scavenge most of their Hg(II) from above the boundary layer.<sup>37</sup> Using scavenging efficiencies from that work and Hg(II) profiles from recent aircraft campaigns,<sup>10,12,35</sup> the free troposphere could contribute 80–90% of Hg deposition in thunderstorms. In addition, the downdrafts and clear-air subsidence induced by thunderstorms can mix Hg(II) to lower altitudes, a process that has been observed for ozone,<sup>38</sup> where it is more readily available for scavenging later. Near large anthropogenic surface Hg(II) sources, however, thunderstorm scavenging from the boundary layer could be more important than is seen at our study sites.<sup>39–41</sup> An upper-troposphere source of Hg in thunderstorms is also consistent

with the steady Hg wet deposition in the southeast United States, in contrast to declines in other regions as national Hg emissions have fallen.<sup>3,6,24</sup>

Further evidence for an important high-altitude source of Hg(II) comes from the ground-level measurements of gaseous and fine particle-bound Hg(II). Mean summer concentrations measured at Pensacola are  $4.1 \pm 3.0$   $\text{pg m}^{-3}$  (Table S2). Although concentrations tend to be slightly ( $0.6$   $\text{pg m}^{-3}$ ) lower during thunderstorms than other rain events, they are statistically indistinguishable between different storm types ( $P = 0.21$ ; Table S2), so below-cloud scavenging cannot explain the higher Hg concentrations in rainwater from thunderstorms. Hg(II) concentrations in Pensacola are lowest under sustained marine flow ( $3.1$   $\text{pg m}^{-3}$ ), highest under continental flow ( $6.0$   $\text{pg m}^{-3}$ ), and intermediate under diurnally alternating land–sea breezes ( $5.0$   $\text{pg m}^{-3}$ ).<sup>42</sup> Despite the land–ocean contrast in Hg(II) concentrations and varying distance to the coast, there are no significant differences in Hg deposition among the four Pensacola sites. The Hg(II) measurements above exclude coarse aerosols, particularly sea salt aerosols that can absorb gaseous Hg(II).<sup>43</sup> Limited observations have found  $3.0$ – $4.6$   $\text{pg m}^{-3}$  in coarse aerosols at the Pensacola site, which is 25 km from the ocean,<sup>26</sup> and  $15$ – $25$   $\text{pg m}^{-3}$  in bulk (fine plus coarse) aerosols on Florida beaches,<sup>26,44</sup> so mean total (gaseous and all particulate) Hg(II) may be  $10$ – $20$   $\text{pg m}^{-3}$  at Pensacola sites. Cloud base altitudes for Florida storms are typically around 1000 m, so the mean vertically integrated Hg(II) that can be scavenged is likely not more than  $20$   $\text{ng m}^{-2}$  in summer because coarse aerosol concentrations usually decrease rapidly with altitude. If all of this Hg(II) is scavenged by precipitation and deposited, the below-cloud Hg(II) would contribute 5–15% of the mean deposition per event at Pensacola, which is  $250 \pm 200$   $\text{ng m}^{-2}$  in thunderstorms and  $130 \pm 100$   $\text{ng m}^{-2}$  in other rain events (Table 1, S3). From literature review,<sup>18,19,45–48</sup> mean summer concentrations of Hg(II) that can be scavenged at the Georgia, Wisconsin, and Vermont sites in this study are likely  $6$ – $13$   $\text{pg m}^{-3}$  (Table S4), which is less than at Pensacola because inland sites lack sea salt aerosols. These ground-level concentrations imply about  $6$ – $13$   $\text{pg m}^{-2}$  below cloud base, which is less than 10% of the mean Hg deposition per event ( $160$ – $200$   $\text{ng m}^{-2}$ , Table 1) at sites outside Florida. Nevertheless, below-cloud Hg scavenging is likely significant at our study sites when surface Hg(II) concentrations are well above their summer average and at other sites that are close to Hg(II) emission sources.<sup>40</sup> Convergence of the horizontal wind into the cloud base could increase the boundary-layer contribution, but, as discussed above, the low-level radar reflectivity, which is associated with moisture convergence, is uncorrelated with Hg concentration in rainwater. The radar and scavengable Hg(II) data are thus inconsistent with a dominant Hg(II) source in the boundary layer.

**3.3. Regional Differences in Hg Deposition.** Deposition is the product of precipitation amount, which is measured, and Hg concentration, which is measured and statistically modeled with eq 1. Following a derivation given in Supporting Information, the statistical model predicts that total summer deposition at each site is approximately

$$\hat{D} \approx \beta_0 p_t \bar{c} (1 + f\beta_2) \quad (2)$$

where  $p_t$  is the total summer precipitation,  $f$  is the fraction of precipitation that comes from thunderstorms,  $\bar{c} = (\bar{p}/p_0)^{\beta_1}$  is a characteristic dilution factor derived from the mean precip-

Table 3. Observed and Predicted Summer Mercury Wet Deposition and Its Components

	site value <sup>a</sup>				deposition ratio <sup>b</sup>			
	Florida <sup>c</sup>	Georgia	Vermont	Wisconsin	FL/VT	FL/WI	FL/GA	WI/VT
component of predicted wet deposition								
mean precipitation depth	21.3 ± 4.6 mm	14.9 ± 4.2 mm	18.1 ± 4.5 mm	18.7 ± 9.1 mm	0.95 ± 0.09	0.96 ± 0.14	0.90 ± 0.09	0.99 ± 0.16
total summer precipitation	500 ± 60 mm <sup>e</sup>	310 ± 73 mm	450 ± 90 mm <sup>e</sup>	410 ± 200 mm	1.11 ± 0.26 <sup>e</sup>	1.22 ± 0.61	1.61 ± 0.42	0.91 ± 0.48
thunderstorm frequency	92 ± 4%	72 ± 11%	48 ± 12%	88 ± 5%	1.17 ± 0.06	1.01 ± 0.02	1.07 ± 0.04	1.16 ± 0.06
baseline concentration	21.8 ± 1.3 ng L <sup>-1</sup>	22.6 ± 1.8 ng L <sup>-1</sup>	15.2 ± 0.9 ng L <sup>-1</sup>	19.3 ± 1.4 ng L <sup>-1</sup>	1.43 ± 0.12	1.13 ± 0.11	0.96 ± 0.10	1.27 ± 0.12
predicted wet deposition <sup>d</sup>	6.5 ± 1.1 μg m <sup>-2</sup>	4.3 ± 1.2 μg m <sup>-2</sup>	3.6 ± 0.9 μg m <sup>-2</sup>	4.8 ± 2.5 μg m <sup>-2</sup>	1.78 ± 0.48 <sup>e</sup>	1.34 ± 0.72	1.50 ± 0.45	1.32 ± 0.74
observed wet deposition	5.7 ± 0.8 μg m <sup>-2</sup>	3.9 ± 0.3 μg m <sup>-2</sup>	4.0 ± 1.1 μg m <sup>-2</sup>	4.8 ± 1.9 μg m <sup>-2</sup>	1.43 ± 0.31	1.19 ± 0.50	1.46 ± 0.23	1.20 ± 0.57
					1.4–3.0 <sup>f</sup>			

<sup>a</sup>Mean and interannual variability (SD). <sup>b</sup>For observed and predicted wet deposition, deposition ratios are the simple division of site values with uncertainty propagation.<sup>53</sup> For each component of predicted wet deposition, ratios are the expected deposition ratio between sites  $x$  and  $y$  if all else were equal (see section 3.3 and in the [Supporting Information](#)): mean precipitation depth,  $(\bar{p}_x/\bar{p}_y)^{\beta_1}$ ; total summer precipitation,  $p_{t,x}/p_{t,y}$ ; thunderstorm frequency or fraction,  $(1 + f_x\beta_2)/(1 + f_y\beta_2)$ ; and baseline concentration,  $\beta_{0,x}/\beta_{0,y}$ . <sup>c</sup>Florida values based on FL96. <sup>d</sup>Predicted from components using eq 2. <sup>e</sup>Total summer precipitation during 2006–2011 was 130 mm less than the 20 year climate mean in Pensacola, FL and 30 mm greater than in Burlington, VT (see the [Supporting Information](#)). Using the climatic-mean total precipitation would predict a FL/VT deposition ratio of  $1.50 \pm 0.35$  for that component alone, instead of 1.11, and the overall predicted FL/VT deposition ratio would be  $2.40 \pm 0.65$ . <sup>f</sup>Range reported in literature from other MDN sites in the Southeast and Northeast United States in summer.<sup>2,3,8</sup>

itation depth ( $\bar{p}$ ), and parameters  $\beta_i$  ( $i = 0, 1, 2$ ) are from the regression fit (Table 2). All terms in eq 2 are site-specific except  $\beta_1$  and  $\beta_2$ .

Table 3 shows that the predicted Hg deposition from eq 2 and the predicted interannual variability are within the observed range at all sites. The regression model further enables us to attribute the deposition ratio between two sites to the components of eq 2: baseline concentration, total precipitation, characteristic dilution based on mean precipitation depth, and thunderstorm frequency. Table 3 provides the deposition ratios that would be expected from each of these components acting alone, all else being equal. Formulas for these components are given in a footnote and in the [Supporting Information](#). We can thus determine which meteorological ( $p$ ,  $\bar{p}$ , and  $f$ ) and chemical ( $\beta_0$ ) factors explain the observed deposition differences between sites.

Over the years of 2006–2011, Hg deposition in Pensacola, Florida was  $43 \pm 31\%$  (a ratio of  $1.43 \pm 0.31$  in Table 3) greater than in Vermont. Observations at our study sites show that Pensacola receives 92% of its summer precipitation from thunderstorms, while Vermont receives just 48% from such storms (Table 3). This effect alone would predict  $17 \pm 6\%$  greater Hg deposition in Florida if precipitation and baseline concentrations were otherwise the same (uncertainty is interannual SD combined with regression parameter SE). Pensacola also has greater average rainfall in each event than does Vermont (21.3 versus 18.1 mm), which decreases deposition  $5 \pm 9\%$ , and greater total summer precipitation (500 versus 450 mm/summer), which increases Florida deposition  $11 \pm 26\%$  (the large range due to large interannual SD in total summer rainfall). Together, the thunderstorm frequency and rain distribution predict  $23 \pm 26\%$  greater summer deposition in Florida than in Vermont, compared to an observed summer deposition difference of  $43 \pm 31\%$ . Precipitation meteorology can thus explain half of the observed difference in Hg deposition between the Vermont and Florida sites in summer. The remaining half of the difference is due to the atmospheric chemistry, emissions, and transport that

generates higher baseline concentrations in Florida. Adding the baseline concentration term to the precipitation factors predicts  $78 \pm 48\%$  higher deposition in Florida, which is consistent with the observed magnitude and interannual range at our sites and at the low end of ratios 1.4–3.0 (40–200%) reported in literature for other sites in the southeast versus the northeast.<sup>2,3,8</sup> Our study years (2006–2011) were unusually dry in Pensacola and unusually wet in Vermont; eq 2 predicts that a return to climate-normal precipitation at these sites would boost the summer deposition ratio to 2.4 (see the [Supporting Information](#)), which is in the middle range of recent literature. The regression approach does not identify why baseline concentrations differ between Florida and Vermont, but there is mounting evidence that elevated Hg(II) concentrations are found in the free troposphere over the South and Southeast of the United States due to oxidation of Hg(0) in the upper troposphere, followed by subsidence in the subtropics.<sup>11,12,49–51</sup>

Table 3 explains the summer deposition differences between other pairs of sites as well. The Florida sites have  $20 \pm 50\%$  greater Hg deposition than the Wisconsin site. The statistical model reproduces this difference ( $34 \pm 72\%$ ) and attributes it mainly to the greater precipitation depth in Florida (500 versus 410 mm implies 22% greater deposition, with the large range mainly due to precipitation variability in Wisconsin), and secondarily to baseline concentrations being higher in Florida (21.8 versus 19.3 ng L<sup>-1</sup> implies 13% greater deposition). Similarly, the Georgia site has lower deposition than did Florida, which is almost entirely because of precipitation depth (500 versus 310 mm implies 60% greater deposition) due to the fact that baseline concentrations and thunderstorm frequency are similar at these sites in the Southeast. The Wisconsin site also has  $20 \pm 57\%$  greater deposition than the Vermont site. For this pair, the deposition ratio is due to higher baseline concentrations in Wisconsin (19.3 versus 15.2 ng L<sup>-1</sup> implies 27% greater deposition) and more-frequent thunderstorms in Wisconsin (88 versus 48% of precipitation implies 16% greater deposition), which are partially offset by the

greater summer precipitation in Vermont (410 versus 450 mm implies 9% less deposition).

Our results support the hypothesis that thunderstorms are particularly effective at scavenging this Hg(II) from the free troposphere, resulting in precipitation Hg concentration and deposition that is nearly 50% greater than in other storms of the same precipitation depth; the connection with thunderstorms is thus not a seasonal coincidence. Thunderstorms may also raise baseline Hg concentrations in nonconvective precipitation by mixing Hg(II) down to lower altitudes where it can be scavenged by all precipitation types. These results pose a challenge for modeling the fate and deposition of atmospheric mercury because the large-scale models that can simulate the global dispersion and oxidation of mercury currently do not explicitly resolve convective precipitation.<sup>3,50,52</sup>

## ■ ASSOCIATED CONTENT

### 📄 Supporting Information

The Supporting Information is available free of charge on the ACS Publications website at DOI: 10.1021/acs.est.6b02586.

Details on the linear version of the statistical model, attribution of regional deposition to meteorological and chemical factors, and precipitation climatology in Vermont and Florida. Figures showing anthropogenic emissions of gaseous and particle-bound Hg(II) in 2011, annual precipitation and terrain elevation in the eastern United States, and distribution of summer precipitation depth. Tables showing site locations and meteorological data sources, concentrations of measured atmospheric mercury species, mean ( $\pm$  SD) summer Hg deposition per rain event ( $\text{ng m}^{-2}$ ), and summer concentrations ( $\text{pg m}^{-3}$ ) of scavengable Hg(II) species at precipitation collection sites. Logarithm of statistical model eq 1 and derivation of eq 2. (PDF)

## ■ AUTHOR INFORMATION

### Corresponding Author

\*Tel: +1-850-645-0972; e-mail: cdholmes@fsu.edu.

### Notes

The authors declare no competing financial interest.

## ■ ACKNOWLEDGMENTS

Tanner Martin, Nathaniel Davila, Autum Dunn, Melissa Overton, Sara Nolek, and Kathleen Gosnell helped with precipitation sample collection and analysis. Sikha Bagui, Jessie Brown, and Alex Maestre assisted with wet deposition database development. We gratefully acknowledge the MDN coordinators and site operators. This work was financially supported by the U.S. Environmental Protection Agency (EPA, Cooperative Agreement X-97455002), the Electric Power Research Institute (EPRI, P27302 C12974), and startup funds from Florida State University. The views, opinions and findings of this paper are those of the authors and should not be construed as an official U.S. EPA or NOAA position or policy.

## ■ REFERENCES

- (1) National Atmospheric Deposition Program (NADP) and Mercury Deposition Network (MDN). MDN Data Retrieval Options. <http://nadp.sws.uiuc.edu/data/MDN/> (accessed June 17, 2013).
- (2) Prestbo, E. M.; Gay, D. A. Wet deposition of mercury in the US and Canada, 1996–2005: Results and analysis of the NADP mercury

deposition network (MDN). *Atmos. Environ.* **2009**, *43* (27), 4223–4233.

- (3) Zhang, Y.; Jaeglé, L. Decreases in Mercury Wet Deposition over the United States during 2004–2010: Roles of Domestic and Global Background Emission Reductions. *Atmosphere* **2013**, *4* (2), 113–131.

- (4) United States Environmental Protection Agency (EPA). National Emissions Inventory. <https://www.epa.gov/air-emissions-inventories> (accessed June 17, 2013).

- (5) Zhang, Y.; Jaeglé, L.; van Donkelaar, A.; Martin, R. V.; Holmes, C. D.; Amos, H. M.; Wang, Q.; Talbot, R.; Artz, R.; Brooks, S.; et al. Nested-grid simulation of mercury over North America. *Atmos. Chem. Phys.* **2012**, *12* (14), 6095–6111.

- (6) Butler, T. J.; Cohen, M. D.; Vermeylen, F. M.; Likens, G. E.; Schmeltz, D.; Artz, R. S. Regional precipitation mercury trends in the eastern USA, 1998–2005: Declines in the Northeast and Midwest, no trend in the Southeast. *Atmos. Environ.* **2008**, *42* (7), 1582–1592.

- (7) Guentzel, J. L.; Landing, W. M.; Gill, G. A.; Pollman, C. D. Processes influencing rainfall deposition of mercury in Florida. *Environ. Sci. Technol.* **2001**, *35* (5), 863–873.

- (8) Selin, N. E.; Jacob, D. J. Seasonal and spatial patterns of mercury wet deposition in the United States: Constraints on the contribution from North American anthropogenic sources. *Atmos. Environ.* **2008**, *42* (21), 5193–5204.

- (9) Sillman, S.; Marsik, F. J.; Al-Wali, K. I.; Keeler, G. J.; Landis, M. S. Reactive mercury in the troposphere: Model formation and results for Florida, the northeastern United States, and the Atlantic Ocean. *J. Geophys. Res.* **2007**, *112* (D23), D23305.

- (10) Brooks, S.; Ren, X.; Cohen, M.; Luke, W. T.; Kelley, P.; Artz, R.; Hynes, A.; Landing, W.; Martos, B. Airborne Vertical Profiling of Mercury Speciation near Tullahoma, TN, USA. *Atmosphere* **2014**, *5* (3), 557–574.

- (11) Shah, V.; Jaegle, L.; Gratz, L. E.; Ambrose, J. L.; Jaffe, D. A.; Selin, N. E.; Song, S.; Campos, T. L.; Flocke, F. M.; Reeves, M.; et al. Origin of oxidized mercury in the summertime free troposphere over the southeastern US. *Atmos. Chem. Phys.* **2016**, *16* (3), 1511–1530.

- (12) Gratz, L. E.; Ambrose, J. L.; Jaffe, D. A.; Shah, V. Oxidation of mercury by bromine in the subtropical Pacific free troposphere. *Geophys. Res. Lett.* **2015**, *42*, 10494–10502.

- (13) Weiss-Penzias, P. S.; Gustin, M. S.; Lyman, S. N. Source of gaseous oxidized mercury and mercury dry deposition at two southeastern U.S. sites. *Atmos. Environ.* **2011**, *45* (27), 4569–4579.

- (14) Cotton, W. R.; Anthes, R. Q. Cumulonimbus clouds and severe convective storms. In *Storm and Cloud Dynamics*; Academic Press: San Diego, CA, 1989.

- (15) Barth, M. C.; Stuart, A. L.; Skamarock, W. C. Numerical simulations of the July 10, 1996, Stratospheric-Tropospheric Experiment: Radiation, Aerosols, and Ozone (STERAO)-Deep Convection experiment storm: Redistribution of soluble tracers. *J. Geophys. Res.-Atmos.* **2001**, *106* (D12), 12381–12400.

- (16) Edgerton, E. S.; Hartsell, B. E.; Jansen, J. J. Mercury speciation in coal-fired power plant plumes observed at three surface sites in the southeastern US. *Environ. Sci. Technol.* **2006**, *40* (15), 4563–4570.

- (17) Landing, W. M.; Caffrey, J. M.; Nolek, S. D.; Gosnell, K. J.; Parker, W. C. Atmospheric wet deposition of mercury and other trace elements in Pensacola, Florida. *Atmos. Chem. Phys.* **2010**, *10*, 4867–4877.

- (18) Engle, M. A.; Tate, M. T.; Krabbenhoft, D. P.; Schauer, J. J.; Kolker, A.; Shanley, J. B.; Bothner, M. H. Comparison of atmospheric mercury speciation and deposition at nine sites across central and eastern North America. *J. Geophys. Res.* **2010**, *115*, D18306.

- (19) Huang, J.; Chang, F.-C.; Wang, S.; Han, Y.-J.; Castro, M.; Miller, E.; Holsen, T. M. Mercury wet deposition in the eastern United States: characteristics and scavenging ratios. *Environ. Sci.: Processes Impacts* **2013**, *15* (12), 2321–2328.

- (20) Driscoll, C. T.; Mason, R. P.; Chan, H. M.; Jacob, D. J.; Pirrone, N. Mercury as a Global Pollutant: Sources, Pathways, and Effects. *Environ. Sci. Technol.* **2013**, *47*, 4967–4983.

- (21) Gustin, M. S.; Weiss-Penzias, P. S.; Peterson, C. Investigating sources of gaseous oxidized mercury in dry deposition at three sites across Florida, USA. *Atmos. Chem. Phys.* **2012**, *12* (19), 9201–9219.
- (22) Caffrey, J. M.; Landing, W. M.; Nolek, S. D.; Gosnell, K. J.; Bagui, S. S.; Bagui, S. C. Atmospheric deposition of mercury and major ions to the Pensacola (Florida) watershed: spatial, seasonal, and inter-annual variability. *Atmos. Chem. Phys.* **2010**, *10*, 5425–5434.
- (23) Risch, M. R.; Gay, D. A.; Fowler, K. K.; Keeler, G. J.; Backus, S. M.; Blanchard, P.; Barres, J. A.; Dvonch, J. T. Spatial patterns and temporal trends in mercury concentrations, precipitation depths, and mercury wet deposition in the North American Great Lakes region, 2002–2008. *Environ. Pollut.* **2012**, *161*, 261–271.
- (24) Weiss-Penzias, P. S.; Gay, D. A.; Brigham, M. E.; Parsons, M. T.; Gustin, M. S.; ter Schure, A. Trends in mercury wet deposition and mercury air concentrations across the U.S. and Canada. *Sci. Total Environ.* **2016**, 1–11.
- (25) Gratz, L. E.; Keeler, G. J. Sources of mercury in precipitation to Underhill, VT. *Atmos. Environ.* **2011**, *45* (31), 5440–5449.
- (26) Engle, M.; Tate, M.; Krabbenhoft, D.; Kolker, A.; Olson, M.; Edgerton, E.; DeWild, J.; McPherson, A. Characterization and cycling of atmospheric mercury along the central US Gulf Coast. *Appl. Geochem.* **2008**, *23* (3), 419–437.
- (27) Knapp, K. R.; Ansari, S.; Bain, C. L.; Bourassa, M. A.; Dickinson, M. J.; Funk, C.; Helms, C. N.; Hennon, C. C.; Holmes, C. D.; Huffman, G. J.; et al. Globally gridded satellite observations for climate studies. *Bull. Am. Meteorol. Soc.* **2011**, *92* (7), 893–907.
- (28) Crum, T. D.; Albery, R. L. The WSR-88D and the WSR-88D Operational Support Facility. *Bull. Am. Meteorol. Soc.* **1993**, *74* (9), 1669–1687.
- (29) Klazura, G. E.; Imy, D. A. A Description of the Initial Set of Analysis Products Available from the NEXRAD WSR-88D System. *Bull. Am. Meteorol. Soc.* **1993**, *74* (7), 1293–1311.
- (30) Jaffrezo, J.-L.; Colin, J.-L.; Gros, J.-M. Some physical factors influencing scavenging ratios. *Atmos. Environ., Part A* **1990**, *24* (12), 3073–3083.
- (31) Savoie, D. L.; Prospero, J. M.; Nees, R. T. Washout ratios of nitrate, non-sea-salt sulfate and sea-salt on Virginia key, Florida and on American Samoa. *Atmos. Environ.* **1987**, *21* (1), 103–112.
- (32) Gratz, L. E.; Keeler, G. J.; Miller, E. K. Long-term relationships between mercury wet deposition and meteorology. *Atmos. Environ.* **2009**, *43* (39), 6218–6229.
- (33) Shanley, J. B.; Engle, M. A.; Scholl, M.; Krabbenhoft, D. P.; Brunette, R.; Olson, M. L.; Conroy, M. E. High mercury Wet deposition at a “clean air” site in Puerto Rico. *Environ. Sci. Technol.* **2015**, *49* (20), 12474–12482.
- (34) Weiss-Penzias, P.; Amos, H. M.; Selin, N. E.; Gustin, M. S.; Jaffe, D. A.; Obrist, D.; Sheu, G. R.; Giang, A. Use of a global model to understand speciated atmospheric mercury observations at five high-elevation sites. *Atmos. Chem. Phys.* **2015**, *15* (3), 1161–1173.
- (35) Lyman, S. N.; Jaffe, D. A. Formation and fate of oxidized mercury in the upper troposphere and lower stratosphere. *Nat. Geosci.* **2012**, *5* (2), 114–117.
- (36) Swartzendruber, P. C.; Jaffe, D. A.; Prestbo, E. M.; Weiss-Penzias, P.; Selin, N. E.; Park, R.; Jacob, D. J.; Strode, S.; Jaegle, L. Observations of reactive gaseous mercury in the free troposphere at the Mount Bachelor Observatory. *J. Geophys. Res.* **2006**, *111*, D24301.
- (37) Nair, U. S.; Wu, Y.; Holmes, C. D.; ter Schure, A.; Kallos, G.; Walters, J. T. Cloud-resolving simulations of mercury scavenging and deposition in thunderstorms. *Atmos. Chem. Phys.* **2013**, *13*, 10143–10157.
- (38) Pan, L. L.; Homeyer, C. R.; Honomichl, S.; Ridley, B. A.; Weisman, M.; Barth, M. C.; Hair, J. W.; Fenn, M. A.; Butler, C.; Diskin, G. S.; et al. Thunderstorms enhance tropospheric ozone by wrapping and shedding stratospheric air. *Geophys. Res. Lett.* **2014**, *41* (22), 7785–7790.
- (39) Dvonch, J. T.; Keeler, G. J.; Marsik, F. J. The influence of meteorological conditions on the wet deposition of mercury in southern Florida. *J. Appl. Meteorol.* **2005**, *44* (9), 1421–1435.
- (40) White, E. M.; Keeler, G. J.; Landis, M. S. Spatial Variability of Mercury Wet Deposition in Eastern Ohio: Summertime Meteorological Case Study Analysis of Local Source Influences. *Environ. Sci. Technol.* **2009**, *43* (13), 4946–4953.
- (41) Lamborg, C. H.; Engstrom, D. R.; Fitzgerald, W. F.; Balcom, P. H. Apportioning global and non-global components of mercury deposition through Pb-210 indexing. *Sci. Total Environ.* **2013**, *448*, 132–140.
- (42) Wu, Y.; Nair, U. S.; Walters, J. T.; Jansen, J. J.; Edgerton, E. S. Characterization of ambient mercury concentration at a coastal site under marine, continental, and land-sea breeze flow regimes; 13th Conference on Atmospheric Chemistry, American Meteorological Society Annual Meeting; Seattle, 2011.
- (43) Holmes, C. D.; Jacob, D. J.; Mason, R. P.; Jaffe, D. A. Sources and deposition of reactive gaseous mercury in the marine atmosphere. *Atmos. Environ.* **2009**, *43*, 2278–2285.
- (44) Malcolm, E.; Keeler, G.; Landis, M. The effects of the coastal environment on the atmospheric mercury cycle. *J. Geophys. Res.* **2003**, *108* (D12) DOI: [10.1029/2002JD003084](https://doi.org/10.1029/2002JD003084).
- (45) Lan, X.; Talbot, R.; Castro, M.; Perry, K.; Luke, W. Seasonal and diurnal variations of atmospheric mercury across the US determined from AMNet monitoring data. *Atmos. Chem. Phys.* **2012**, *12* (21), 10569–10582.
- (46) Nair, U. S.; Wu, Y.; Walters, J.; Jansen, J.; Edgerton, E. S. Diurnal and seasonal variation of mercury species at coastal-suburban, urban, and rural sites in the southeastern United States. *Atmos. Environ.* **2012**, *47*, 499–508.
- (47) Landis, M.; Keeler, G. Atmospheric mercury deposition to Lake Michigan during the Lake Michigan Mass Balance Study. *Environ. Sci. Technol.* **2002**, *36* (21), 4518–4524.
- (48) Cheng, I.; Zhang, L.; Mao, H. Relative contributions of gaseous oxidized mercury and fine and coarse particle-bound mercury to wet deposition at nine monitoring sites in North America. *J. Geophys. Res.-Atmos.* **2015**, *120*, 8549–8562.
- (49) Coburn, S.; Dix, B.; Edgerton, E.; Holmes, C. D.; Kinnison, D.; Liang, Q.; ter Schure, A.; Wang, S.; Volkamer, R. Mercury oxidation from bromine chemistry in the free troposphere over the southeastern US. *Atmos. Chem. Phys.* **2016**, *16* (6), 3743–3760.
- (50) Holmes, C. D.; Jacob, D. J.; Corbitt, E. S.; Mao, J.; Yang, X.; Talbot, R.; Slemr, F. Global atmospheric model for mercury including oxidation by bromine atoms. *Atmos. Chem. Phys.* **2010**, *10* (24), 12037–12057.
- (51) Wang, S.; Schmidt, J. A.; Baidar, S.; Coburn, S.; Dix, B.; Koenig, T. K.; Apel, E.; Bowdalo, D.; Campus, T. L.; Eloranta, E.; et al. Active and widespread halogen chemistry in the tropical and subtropical free troposphere. *Proc. Natl. Acad. Sci. U. S. A.* **2015**, *112* (30), 9281–9286.
- (52) Bullock, O. R.; Atkinson, D.; Braverman, T.; Civerolo, K.; Dastoor, A.; Davignon, D.; Ku, J.-Y.; Lohman, K.; Myers, T. C.; Park, R. J.; et al. An analysis of simulated wet deposition of mercury from the North American Mercury Model Intercomparison Study. *J. Geophys. Res.* **2009**, *114* (D8), D08301.
- (53) Taylor, J. R. Propagation of uncertainties. In *An Introduction to Error Analysis*, 2nd ed.; University Science Books: Sausalito, CA, 1997; pp 45–92.

#### NOTE ADDED AFTER ASAP PUBLICATION

This paper was published ASAP on August 24, 2016 with incorrect units in Table 3 and other minor text errors. The corrected version was reposted on August 25, 2016.